ACS Catalysis

pubs.acs.org/acscatalysis

Research Article

Biomimetic Dehydroamination of Primary Amines

Chenyang Wang, Phong Dam, Mohamed Elghobashy, Angelika Brückner, Jabor Rabeah, Luis Miguel Azofra, and Osama El-Sepelgy*

Cite This: ACS Catal. 2023, 13, 14205−14212

Read Online

ACCESS | Metrics & More | Article Recommendations | Supporting Information

ABSTRACT: Herein, we present a biomimetic method for the catalytic deammoniation of diverse primary amines, including amino acids, natural products, and pharmaceuticals. This innovative approach, characterized by its operational simplicity and high selectivity, provides a rapid and easily accessible pathway to a wide range of olefin products derived from nonfossil-based chemicals. The transformation relies on the utilization of two readily available photoactive catalysts: acridinium salt and cobaloxime. Through a combination of experimental and theoretical studies, we have gained valuable insights into the fundamental steps underlying this unconventional dehydroamination process.

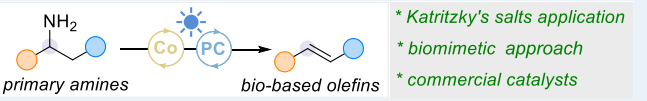

KEYWORDS: *visible light, excited-state, base metals, biomimetic, desaturation*

Biomimetic organic synthesis, inspired by nature's efficient and selective pathways, has emerged as a powerful strategy for the development of novel chemical transformations that mimic enzymatic processes.[1] Deammoniation plays a crucial role in a range of biological processes, including the biosynthesis of natural products and the metabolism of amino acids. For instance, phenylalanine ammonia lyase converts L-phenylalanine to cinnamic acid,[2] a critical precursor for the biosynthesis of lignols, flavonoids, coumarins, aurones, and stilbenes (Scheme 1a).[3]

Despite recent advancements in biomimetic synthesis and the growing interest in replacing fossil-based chemicals with biobased alternatives in the chemical industry, it is surprising that there is a lack of readily available and mild in vitro methods for converting primary amines into alkenes.[4,5] To the best of our knowledge, two classical methods are known for this transformation: Hofmann elimination,[5] which involves exhaustive methylation of primary amines to quaternary ammonium salts, followed by counterion exchange with stoichiometric silver oxide. While Cope elimination[6] involves the oxidation of *t*-amines with peroxides. The production of the alkenes mostly requires harsh thermal and vacuum conditions (Scheme 1b).[7] In addition, unlike alcohols, Burgess reagent proved to be an unsuccessful defunctionalization reagent.[8]

We envisage the feasibility of mimicking the natural reactivity via the development of a nonenzymatic process (Scheme 1c). Our design makes use of the recent progress on the mild generation of C-centered radicals from activated primary amines such as pyridinium salt.[9−11] A major challenge is the subsequent fast reduction of the formed radicals and the generation of the corresponding alkanes.[12] To solve the problem, we decided to employ cobaloxime catalysis, a model of vitamin B12, for the mild conversion of the alkyl radicals to the corresponding olefin.[13] Indeed, this concept draws inspiration from the natural ability of methylcobalamin to act as a reversible free radical carrier that effectively stabilizes highly reactive methyl radicals via the formation of weak carbon−cobalt bonds.[14] Thus, we reported herein the first example of mild dehydroamination of primary amines enabled by a synergistic combination of two photoactive catalysis: organic dye and cobaloxime.[15−17] It is noteworthy that in 1982, Katritzky converted primary amines into tetrahydrobenzoacridium salts, followed by thermolysis at 150−180 °C, yielding the respective olefins.[18]

Our mechanistic proposal is initiated by the generation of *α*-amino radical **A** from *N*,*N*-diisopropylethylamine (*i*-Pr_2NEt) upon the use of highly oxidizing excited-state organic dye such as [Mes-Acr-Me^+]* ($E_{1/2}^{red}$ = +2.06 V vs SCE).[19] The formed *α*-amino radical **A** enables the single electron transfer (SET) reduction of the pyridinium salt, producing the corresponding C-centered radical **B**. Subsequently, the open-shell species **B** are intercepted by a persistent 17-electron $[Co]^{II}$ radical,[20] forming an alkyl-$[Co]^{III}$ intermediate **C** that undergoes C−cobalt bond homolysis upon light irradiation. At this stage, $[Co]^{II}$ performs *α*,*β*-hydrogen abstraction, resulting in the formation of the desired olefin and a $[Co]^{III}$−H species. The cobalt and photoredox catalytic cycles culminate through a simultaneous SET event between the $[Co]^{III}$ intermediate ($E_{1/2}^{red}$ = −0.68 V vs SCE)[21] and the reduced form of the photocatalyst (PC) Mes-Acr-Me•. By employing this envisioned approach, we aim to provide a milder and more

Received: September 11, 2023
Revised: October 4, 2023

https://doi.org/10.1021/acscatal.3c04305
ACS Catal. 2023, 13, 14205−14212

Scheme 1. State-of-the-Art of the Dehydroamination

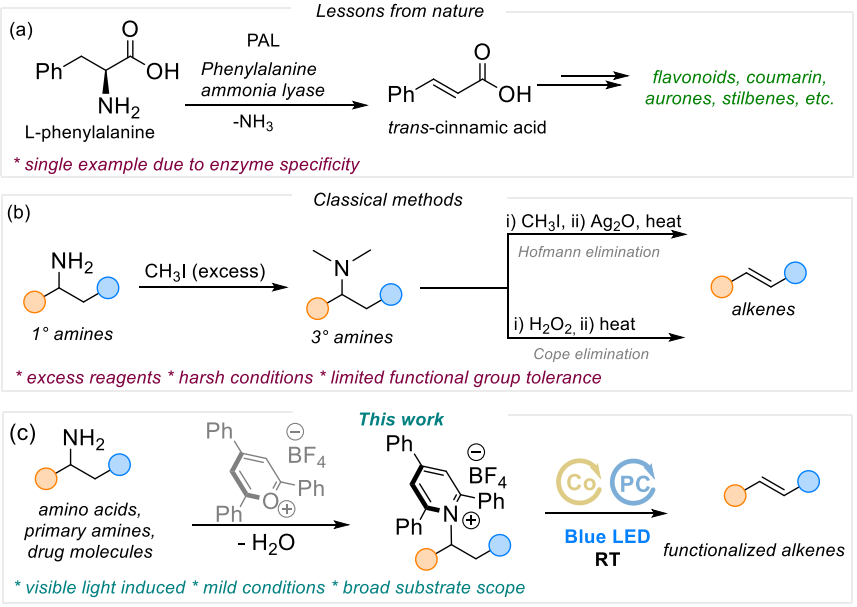

Scheme 2. Our Envisioned Mechanistic Proposal

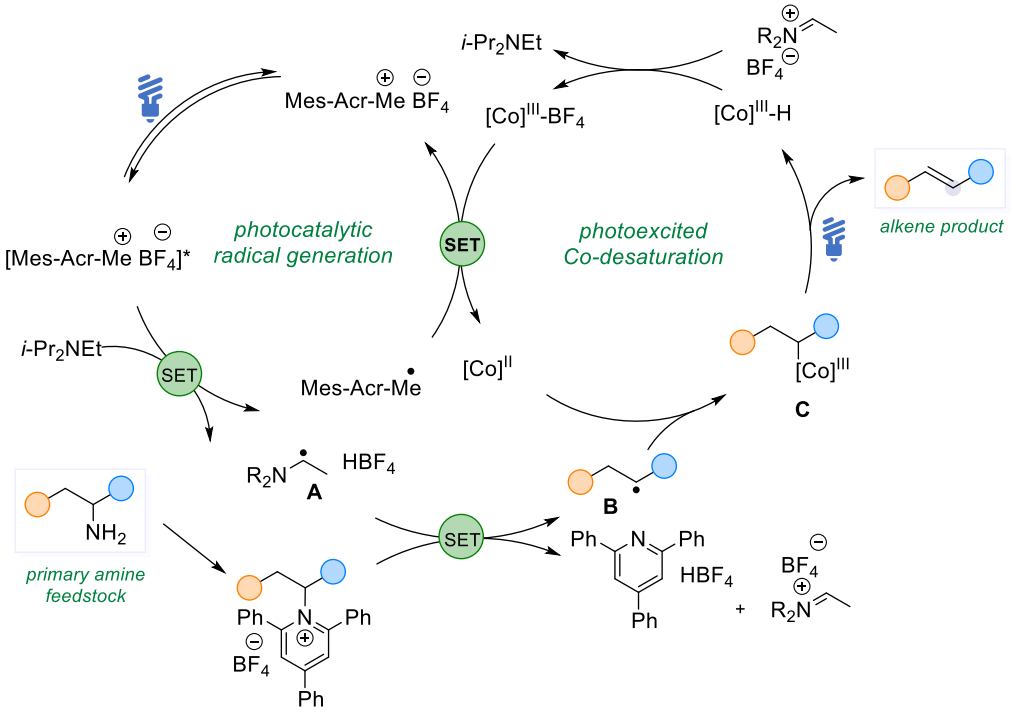

accessible alternative for dehydroamination, contributing to the development of sustainable and efficient synthetic organic chemistry (Scheme 2).

The optimization of the reaction conditions for the synergistic combination of photoredox and cobalt catalysis is summarized in Table 1. Initially, the evaluation focused on essential amino acid derivative **1**, mimicking the transformation by phenylalanine ammonia lyase (Scheme 1a). Optimized conditions applied the use of two commercially available catalysts: Mes-Acr-$MeClO_4$ (1 mol %) and $Co(dmgH)_2PyCl$ ([**Co**]-**1**, 5 mol %). The reaction was carried out in a 0.1 M dichloromethane (DCM) solution with 2 equiv of diisopropylethylamine (*i*-Pr_2NEt) as a base at room temperature, using blue light-emitting diodes for irradiation. This condition yielded the desired methyl cinnamate product **31** in 84% nuclear magnetic resonance (NMR) yield and excellent *E*-selectivity (>20:1) (Table 1, entry 1). The use of Mes-Acr-$MeBF_4$ as a PC led to comparable results (Table 1, entry 2). However, less oxidizing photosensitizers, such as Eosin Y* ($E_{1/2}^{red}$ = +0.83 V vs SCE),[22] 4CzIPN* ($E_{1/2}^{red}$ = +1.35 V vs SCE),[23] and Riboflavin* ($E_{1/2}^{red}$ = +1.50 V vs SCE),[24] resulted in lower product yields (Table 1, entries 3−5). This suggests that the reaction pathway likely involves SET from an electron donor to the excited-state PC. Similar results were obtained when the reaction was conducted in acetonitrile instead of DCM (Table 1, entry 6). Screening of different organic and

https://doi.org/10.1021/acscatal.3c04305
ACS Catal. 2023, 13, 14205−14212

Table 1. Reaction Development[a]

entry	deviation from the standard conditions	yield (%)	E/Z ratio
1	none	84	>20:1
2	Mes-Acr-MeBF$_4$ as PC	82	>20:1
3	Eosin Y as PC	22	>20:1
4	Riboflavin as PC	38	10:1
5	4CzIPN as PC	40	>20:1
6	CH_3CN as solvent	80	>20:1
7	DBU as base	37	>20:1
8	K_2CO_3 as base	Trace	
9	Et_3N as base	30	10:1
10	[**Co**]-**2** instead of [**Co**]-**1**	82	>20:1
11	[**Co**]-**3** (single catalyst)	23	15:1
12	no light/PC/[Co]/base	n.r	

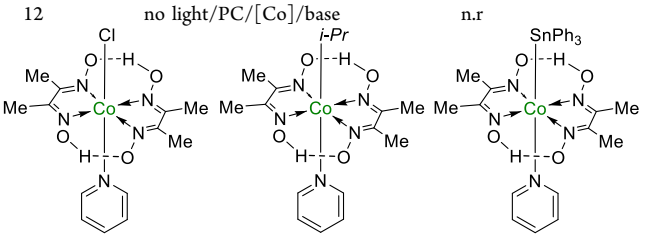

[a]Standard conditions: substrate **1** (0.2 mmol), [**Co**]-**1** (0.005 mmol, 4 mg), Mes-Acr-MeClO$_4$ (0.002 mmol, 0.8 mg), i-Pr$_2$NEt (0.4 mmol, 70 μL), DCM (2 mL), RT, 16 h, NMR yields.

inorganic bases revealed that i-Pr$_2$NEt is the optimal choice (Table 1, entries 7−9). Furthermore, the use of Co(dmgH)$_2$(i-Pr)(py) [**Co**]-**2**[25] resulted in an NMR yield of 82% (Table 1, entry 10). Importantly, the application of the bifunctional [Co]-SnPh$_3$ catalyst [**Co**]-**3** as a single catalyst[26] led to a significant decrease in yield and selectivity (Table 1, entry 11). Finally, we conducted control experiments by individually omitting the PC, [**Co**] catalyst, base, or light. In each instance, no product was detected (Table 1, entry 12).

After establishing optimal conditions, we investigated the dehydroamination of various Katritzky salts[9] (Scheme 3). Our visible-light protocol demonstrated tolerance toward a wide range of primary amines, amino acids, natural products, and drug molecules (**1**−**30**). We initiated the substrate scope exploration with different amino acids, including a variety of common amino acids. Methyl and benzyl phenylalanine derivatives could be transformed to the corresponding cinnamates **31** and **32** with isolated yields of 82% and 85%, respectively. Phenylalanine derivatives bearing electron-withdrawing groups provided the desired α,β-unsaturated esters (**33**−**35**) along with varying amounts of saturated products. Conversely, the electron-rich tyrosine selectively furnished the corresponding *trans*-cinnamate **36**.

Furthermore, homophenylalanine successfully underwent our protocol, yielding ester **37** with an 80% yield and moderate E/Z selectivity. Aliphatic amino acids such as leucine and norleucine readily afforded the corresponding α,β-unsaturated esters **38** and **39** with excellent yields and selectivity. Also, isoleucine yielded the trisubstituted olefin **40** with a high yield and an E/Z ratio of 1.2:1. Notably, the sulfur-containing amino acid methionine could be selectively converted to E-alkene **41** in 71% yield. Aspartic acid and glutamic acid, which are dicarboxylic amino acids, furnished the desired selective E-olefins **42** and **43** with yields of 60 and 71%, respectively. Additionally, the carboxamide-containing amino acid asparagine produced the olefin **44** with an 86% yield and excellent stereocontrol, while glutamine resulted in the unsaturated ester **45** with moderate selectivity. Lysine was successfully converted to alkene **46** in 59% yield with complete selectivity. Furthermore, tryptophan, a heterocyclic-based amino acid, tolerated our system and provided excellent yields and selectivity for products **47** and **48**.

Next, we explored primary amines beyond amino acids. Gratifyingly, 2-aminoindane, a designer drug, yielded indene (**49**) in 70% yield. Amphetamine resulted in a 58% yield mixture of terminal and internal olefins (ratio 2:1) due to the competitive nature of the Co catalyst in abstracting both the reactive benzylic and less hindered terminal hydrogen atoms. In contrast, 4-phenyl-2-butanamine exclusively formed terminal alkene **51**. Cyclic amines were amendable to the reaction, delivering the desired products **52**−**55**. It is worth noting the excellent regioselectivity of the formation of olefin **54**. This highlighting the tendency of the cobaloxime to abstract the less hindered β-hydrogen atom. Gratifyingly, phenylalaninol also delivered cinnamyl alcohol (**56**) in 65% yield. In addition, a testosterone derivative underwent dehydroamination to produce olefin **58**, albeit in a mixture of regioisomers. The cardic drug mexiletine was also converted to its corresponding terminal olefin **59** with moderate regioselectivity. Interestingly, the application of a β-aminoglucose derivative led to the formation of the unsaturated deoxysugar **60** with the elimination of the β-OAc group instead of the β-hydrogen.

To confirm the proposed reaction mechanism of the synergetic photoredox-cobalt catalytic system depicted in Scheme 2, a combination of experimental and theoretical methods was applied. Fluorescence measurements were conducted under inert conditions at room temperature to differentiate between oxidative and reductive quenching of the acridine PC. No quenching of the excited state PC was observed with the substrate and cobaloxime catalyst, while i-Pr$_2$NEt effectively quenched the excited state of the PC, supporting the proposed reductive quenching pathway. Figure 1a shows the Stern−Volmer plot for the fluorescence quenching of Mes-Acr-MeClO$_4$ with i-Pr$_2$NEt. Further electron paramagnetic resonance (EPR) measurements at room temperature of the irradiated [Mes-Acr-Me$^+$ClO$_4$]* did not show any EPR signal. However, a gradual development of a new EPR signal at g = 2.004 was observed with time in the presence of i-Pr$_2$NEt due to the formation of Mes-Acr-Me• (Figure 1b).[27] The formed spectra are in accordance with the theoretical simulation of Mes-Acr-Me• (See Supporting Information for details).

Density functional theory (DFT) calculations shown in Figure 2 supported the fluorescence and EPR results, showing that PC undergoes light-induced vertical (Franck−Condon) excitation to triplet state [**PC**(FC)] at 45.3 kcal/mol. After relaxation, PC transitions to the relaxed triplet state [**PC**(T$_1$)] at 38.4 kcal/mol. The highly oxidizing excited-state species undergoes SET from i-Pr$_2$NEt, leading to the reduction of the acridine PC to the radical Mes-Acr-Me• in the double state. The reductive quenching process is spontaneous, releasing 17.2 kcal/mol. As depicted in Figure 2, the complex of i-

https://doi.org/10.1021/acscatal.3c04305
ACS Catal. 2023, 13, 14205−14212

Scheme 3. Scope of Visible Light Induced Dehydroamination of Primary Amines.[a-c] (See Supporting Information[a])

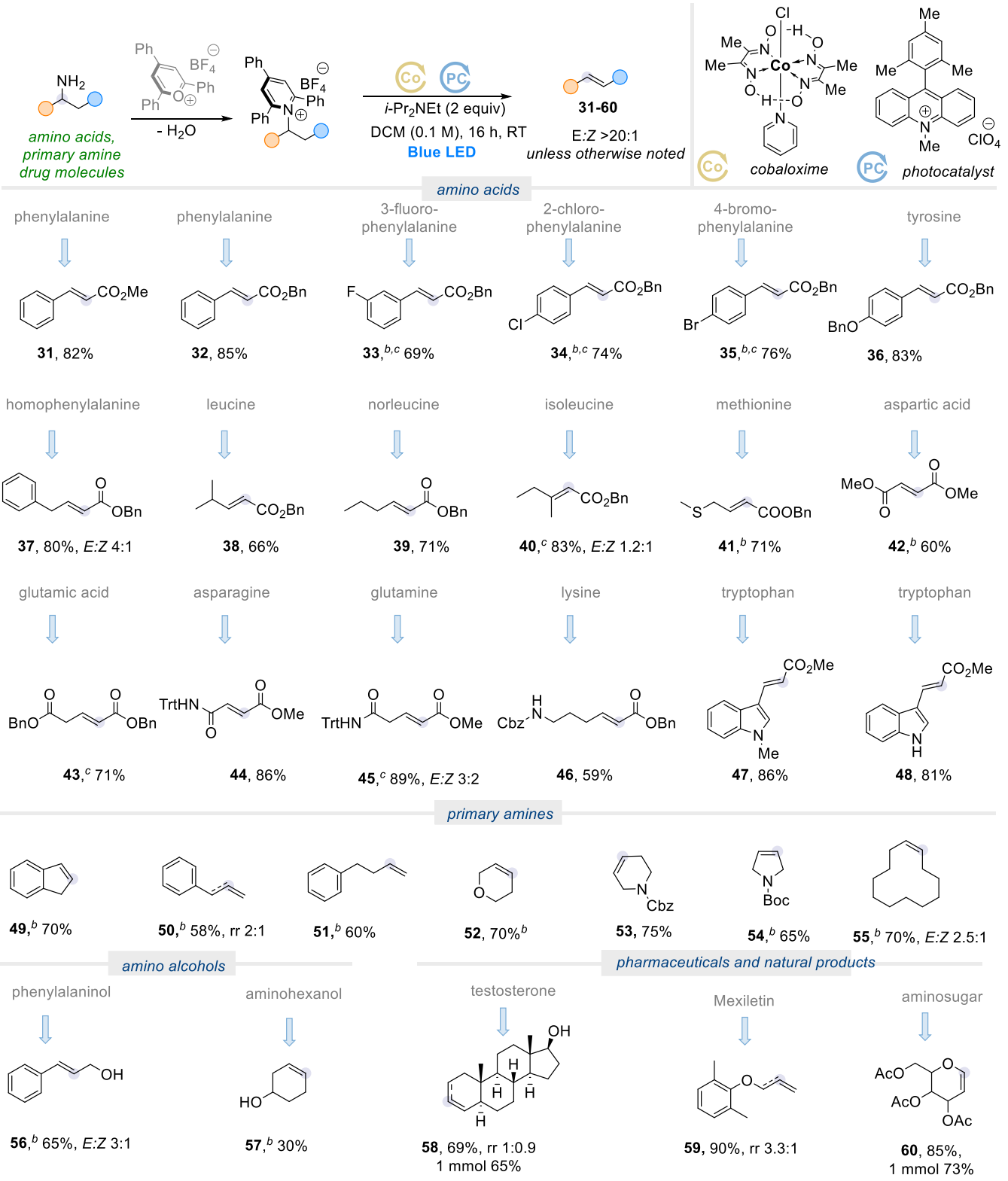

[a]Standard conditions: pyridinium salt (0.2 mmol), [Co]-1 (0.01 mmol, 0.8 mg), Acr-MeClO4 (0.002 mmol, 0.8 mg), i-Pr$_2$NEt (0.4 mmol, 70 μL), DCM (2 mL), RT, 16 h, the reported yields refer to the conversion of the pyridinium salts to the olefins (see supporting information for details). [b]NMR yield. [c]Contains minor amount of hydrodeamination by-product.

$Pr_2NEt^{\bullet+}$ and HBF_4 facilitates the exergonic formation of a carbon-centered radical, releasing 36.5 kcal/mol. Subsequent addition of pyridinium salt **1** to the reaction mixture results in the formation of organic radical intermediate **sub** (D). This was confirmed by a spin trapping experiment using 5,5-dimethyl-1-pyrroline-*N*-oxide (DMPO), resulting in a six-line EPR signal due to the formation of a DMPO-$^{\bullet}$R adduct (Figure 1c). According to the proposed reaction mechanism,

https://doi.org/10.1021/acscatal.3c04305
ACS Catal. 2023, 13, 14205−14212

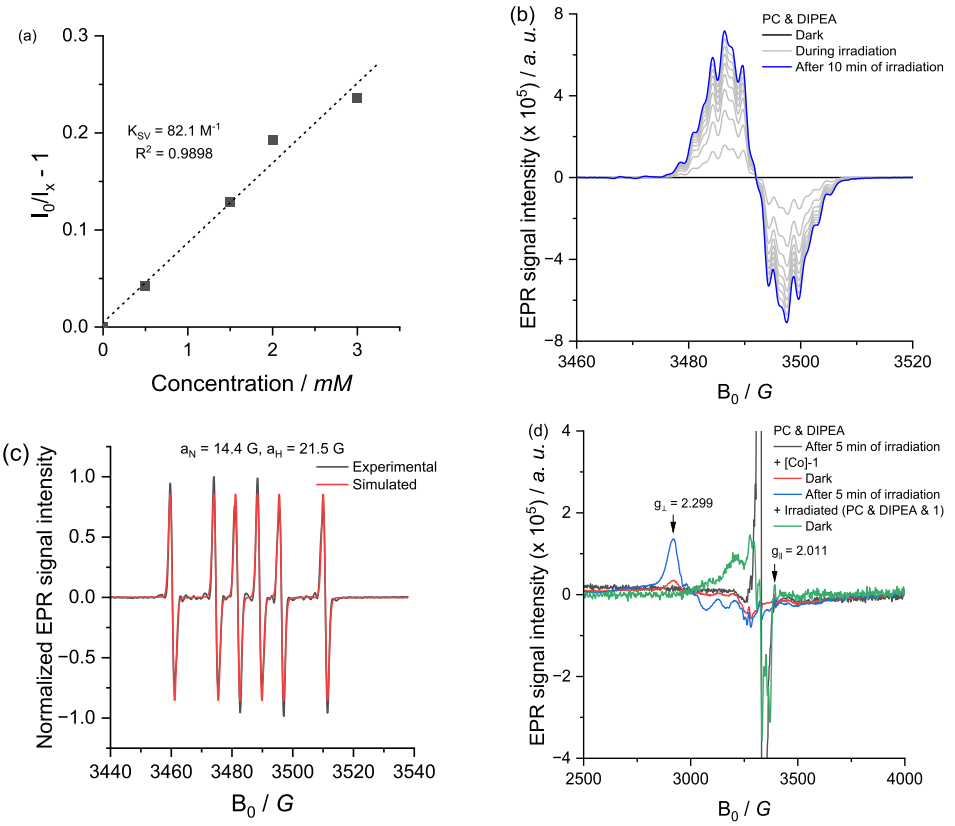

Figure 1. (a) Stern−Volmer plot for fluorescence quenching of Mes-Acr-MeClO$_4$ with *i*-Pr$_2$NEt; (b) EPR spectra recorded at room temperature of the mixture of PC and *i*-Pr$_2$NEt before and after the irradiation; (c) Experimental and simulated EPR spectrum of the irradiated mixture between PC and *i*-Pr$_2$NEt after the addition of substrate and DMPO; (d) EPR spectra recorded at −173 °C of the irradiated mixture of PC and *i*-Pr$_2$NEt with the addition of [**Co**]-**1**, then subsequential addition of the irradiated solution of PC, *i*-Pr$_2$NEt, and substrate.

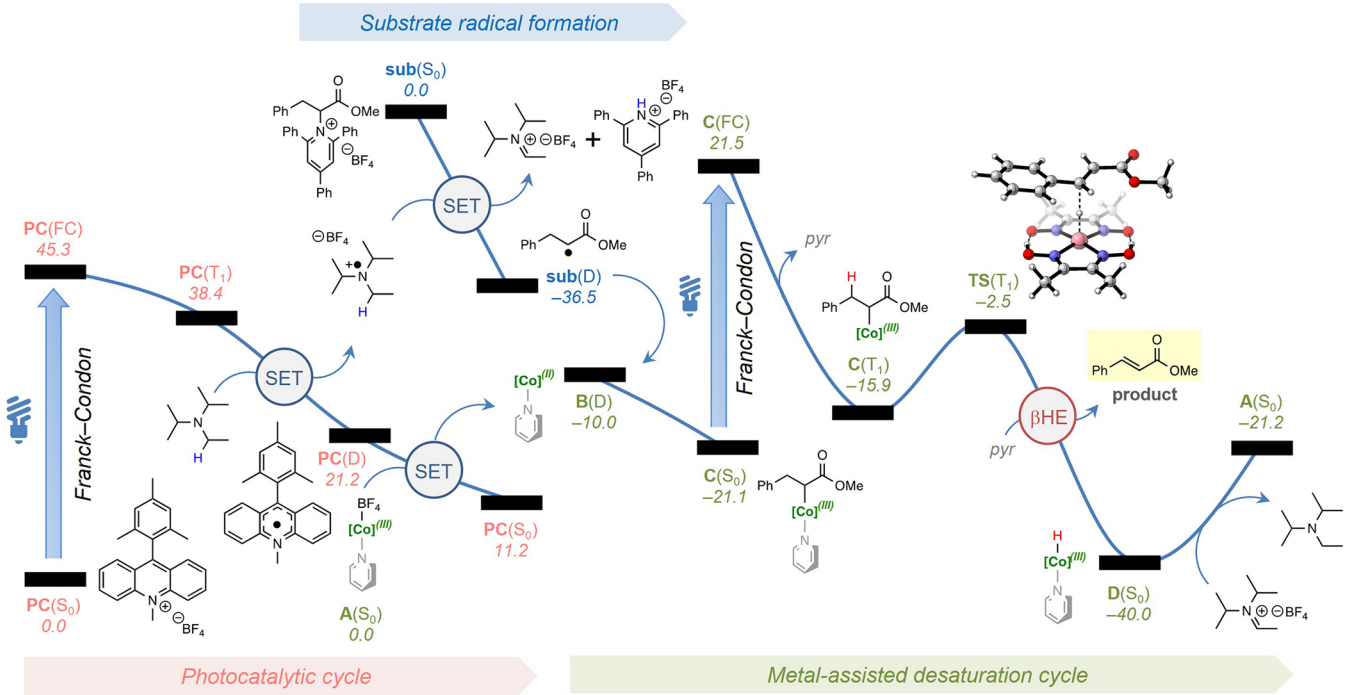

Figure 2. Potential energy surface (PES) for the light-assisted deamination process constituted by the photocatalytic cycle, substrate radical formation, and the metal-assisted desaturation cycle. Free energies (room temperature) are shown in kcal mol^{-1} at the BP91/TZVP//BP91/SVP computational level, using acetonitrile (ε = 35.688) as solvent.

https://doi.org/10.1021/acscatal.3c04305
ACS Catal. 2023, 13, 14205−14212

the organic radical intermediate is trapped by the $[Co]^{II}$ species to form $[Co]^{III}$-substrate. Low-temperature EPR measurements at −173 °C were performed to monitor the [Co] species since it is EPR-inactive at reaction temperature. As we mentioned before, the photocatalytic radical generation cycle results in the formation of a PC radical anion. This radical was also detected at −173 °C, however, with a much higher signal intensity (Figure 1d, black line). Upon the addition of [**Co**]-**1** to PC and *i*-Pr_2NEt mixture, the EPR signal of the reduced PC vanished with time, accompanied by appearing of a new signal at $g_\perp = 2.299$ and $g_\parallel = 2.011$ (Figure 1d, red and blue lines) due to the formation of EPR-active $[Co]^{II}$ species. DFT calculations revealed that this SET process is spontaneous, with an energy release of −10.0 kcal/mol. The presence of pyridinium salt **1** caused the disappearance of the $[Co]^{II}$ signal and the *in-situ*-generated substrate radical due to the formation of EPR-silent $[Co]^{III}$-substrate (Figure 1d, green line). DFT calculations supported the formation of the highly stable complex **C**(S0) at −21.1 kcal/mol (Figure 2). This can be attributed to the photolysis of relatively weak $C(sp^3)-[Co]^{III}$ bonds (BDE < 30 kcal/mol). In more detail, the excitation of $\mathbf{C}(S_0)$ by light leads to the formation of the Franck−Condon triplet state, **C**(FC), and its subsequent relaxation to the triplet state, $\mathbf{C}(T_1)$, accompanied by the release of pyridine. In this spin state, the subsequent elimination of the hydrogen at the β-position occurs, resulting in the desaturation of the substrate and the formation of $[Co]^{III}$-H, $\mathbf{D}(S_0)$, via homolytic cleavage of the $C(sp^3)-[Co]^{III}$ bond. This transition state, $\mathbf{TS}(T_1)$, was located and found to be only 12.8 kcal/mol higher in free energy relative to $\mathbf{C}(T_1)$. Finally, the $[Co]^{III}$-hydride complex regenerates *i*-Pr_2NEt and complex $\mathbf{A}(S_0)$, completing the cycle.

In conclusion, we have reported a straightforward conversion of various primary amines, including amino acids, natural products, and drug molecules, into their respective alkenes with selectivity for the trans-configured isomers. This biomimetic transformation was achieved using a dual organic dye/photoexcited base metal[28] catalysis system under visible light irradiation at room temperature. The protocol offers the flexibility to employ a diverse range of common amino acids and allows for late-stage functionalization of drug molecules. Given its simplicity, effectiveness, mild reaction conditions, and broad applicability, we anticipate that this photocatalytic dehydroamination method will find widespread use in both academic and industrial settings.

■ ASSOCIATED CONTENT

Supporting Information

The Supporting Information is available free of charge at https://pubs.acs.org/doi/10.1021/acscatal.3c04305.

Experimental procedures, analytical data for all new compounds, and NMR spectra (PDF)

■ AUTHOR INFORMATION

Corresponding Author

Osama El-Sepelgy − *Leibniz Institute for Catalysis e.V., Rostock 18059, Germany;* orcid.org/0000-0003-3131-4988; Email: Osama.Elsepelgy@Catalysis.de

Authors

Chenyang Wang − *Leibniz Institute for Catalysis e.V., Rostock 18059, Germany;* orcid.org/0000-0001-6210-4129

Phong Dam − *Leibniz Institute for Catalysis e.V., Rostock 18059, Germany*

Mohamed Elghobashy − *Leibniz Institute for Catalysis e.V., Rostock 18059, Germany*

Angelika Brückner − *Leibniz Institute for Catalysis e.V., Rostock 18059, Germany;* orcid.org/0000-0003-4647-1273

Jabor Rabeah − *Leibniz Institute for Catalysis e.V., Rostock 18059, Germany;* orcid.org/0000-0003-2162-0981

Luis Miguel Azofra − *Instituto de Estudios Ambientales y Recursos Naturales (i-UNAT), Universidad de Las Palmas de Gran Canaria (ULPGC), Las Palmas de Gran Canaria 35017, Spain;* orcid.org/0000-0003-4974-1670

Complete contact information is available at: https://pubs.acs.org/10.1021/acscatal.3c04305

Author Contributions

The manuscript was written through contributions of all authors. All authors have given approval to the final version of the manuscript.

Funding

This work has been financially supported by the Deutsche Forschungsgemeinschaft (DFG, grant number EL 1041/3-1) and by the Leibniz Institute for Catalysis e.V.

Notes

The authors declare no competing financial interest.

■ ACKNOWLEDGMENTS

M.E. thanks the Erasmus Munds program of the EU (SusCat) for the master scholarship. L.M.A. is a Ramón y Cajal fellow (ref RYC2021-030994-I) and thanks MCIN/AEI and NextGenerationEU/PRTR for support. We thank the KAUST Supercomputer Laboratory (KSL), KSA for providing the computational resources (Shaheen II). O.E.-S thanks Prof. Dr. Matthias Beller for his continued generous support.

■ REFERENCES

(1) Erwan, P.; Bastien, N. *Biomimetic Organic Synthesis*; Wiley VCH Verlag GmbH & Co. KGaA, 2021.

(2) Camm, E. L.; Towers, G. H. N. Phenylalanine ammonia lyase. *Phytochemistry* **1973**, *12*, 961−973.

(3) Vogt, T. Phenylpropanoid Biosynthesis. *Mol. Plant* **2010**, *3*, 2−20.

(4) (a) Wohlgemuth, R. Selective Biocatalytic Defunctionalization of Raw Materials. *ChemSusChem* **2022**, *15*, No. e202200402. (b) Berger, K. J.; Levin, M. D. Reframing primary alkyl amines as aliphatic building blocks. *Org. Biomol. Chem.* **2021**, *19*, 11−36. (c) Modak, A.; Maiti, D. Metal catalyzed defunctionalization reactions. *Org. Biomol. Chem.* **2016**, *14*, 21−35.

(5) (a) Schwartz, Z.; Valiton, C.; Lovasz, M.; Roberts, A. G. Recent Applications of Ammonium Ylide Based [2,3]-Sigmatropic and [1,2]-Stevens Rearrangements To Transform Amines into Natural Products. *Synthesis* **2023**. (b) McFadden, T. P.; Nwachukwu, C. I.; Roberts, A. G. An amine template strategy to construct successive C-C bonds: synthesis of benzo[h]quinolines by a deaminative ring contraction cascade. *Org. Biomol. Chem.* **2022**, *20*, 1379−1385.

(6) (a) von Hofmann, A. W. Beitrage zur Kenntniss der fluchtigen organischen Basen. *Ann. Chem. Pharm.* **1851**, *78*, 253−286. (b) Bach, R. D. trans-CYCLOOCTENE. *Org. Synth.* **1969**, *49*, 39. (c) Trauner, D. Richard Willstatter and the 1915 Nobel Prize in Chemistry. *Angew. Chem., Int. Ed.* **2015**, *54*, 11910−11916.

(7) (a) Cope, A. C.; Ciganek, E.; Horning, E. C. Methylenecyclohexane And *N,N*-Dimethylhydroxylamine Hydrochloride. *Org. Synth.* **1959**, *39*, 40. (b) Cope, A. C.; Foster, T. T.; Towle, P. H. Thermal

Decomposition of Amine Oxides to Olefins and Dialkylhydroxylamines. *J. Am. Chem. Soc.* **1949**, *71*, 3929−3934. (c) Serna, A. V.; Kürti, L.; Siitonen, J. H. Synthesis of (±)-Setigerumine I: Biosynthetic Origins of the Elusive Racemic Papaveraceae Isoxazolidine Alkaloids. *Angew. Chem., Int. Ed.* **2021**, *60*, 27236−27240.

(8) (a) Nicolaou, K. C.; Snyder, S. A.; Longbottom, D. A.; Nalbandian, A. Z.; Huang, X. New Uses for the Burgess Reagent in Chemical Synthesis: Methods for the Facile and Stereoselective Formation of Sulfamidates, Glycosylamines, and Sulfamides. *Chem.—Eur. J.* **2004**, *10*, 5581−5606. (b) De Christopher, P. J.; Adamek, J. P.; Lyon, G. D.; Galante, J. J.; Haffner, H. E.; Boggio, R. J.; Baumgarten, R. J. Approach to deamination. III. High-yield conversion of primary aliphatic amines into alkyl halides and alkenes via the use of sulfonimide leaving groups. *J. Am. Chem. Soc.* **1969**, *91*, 2384−2385. (c) Curtis, V. A.; Knutson, F. J.; Baumgarten, R. J. New deaminations IX - pyrolysis of N-alkyl-N,N-disulfonimides. *Tetrahedron Lett.* **1981**, *22*, 199−202.

(9) for reviews; (a) Katritzky, A. R.; Marson, C. M. Pyrylium Mediated Transformations of Primary Amino Groups into Other Functional Groups. New Synthetic Methods. *Angew. Chem., Int. Ed.* **1984**, *23*, 420−429. (b) He, F.-S.; Ye, S.; Wu, J. Recent Advances in Pyridinium Salts as Radical Reservoirs in Organic Synthesis. *ACS Catal.* **2019**, *9*, 8943−8960. (c) Correia, J. T.; Fernandes, V.; Matsuo, B. T.; Delgado, J. A.; de Souza, W. C.; Paixão, M. W. Photoinduced deaminative strategies: Katritzky salts as alkyl radical precursors. *Chem. Commun.* **2020**, *56*, 503−514. (d) Pang, Y.; Moser, D.; Cornella, J. Pyrylium Salts: Selective Reagents for the Activation of Primary Amino Groups in Organic Synthesis. *Synthesis* **2020**, *52*, 489−503. (e) Li, Y.-N.; Xiao, F.; Guo, Y.; Zeng, Y.-F. Recent Developments in Deaminative Functionalization of Alkyl Amines. *Eur. J. Org Chem.* **2021**, *2021*, 1215−1228.

(10) (a) Basch, C. H.; Liao, J.; Xu, J.; Piane, J. J.; Watson, M. P. Harnessing Alkyl Amines as Electrophiles for Nickel-Catalyzed Cross Couplings via C-N Bond Activation. *J. Am. Chem. Soc.* **2017**, *139*, 5313−5316. (b) Klauck, F. J. R.; James, M. J.; Glorius, F. Deaminative Strategy for the Visible-Light-Mediated Generation of Alkyl Radicals. *Angew. Chem. Int. Ed.* **2017**, *56*, 12336−12339.

(11) Selected examples: (a) Hu, J.; Wang, G.; Li, S.; Shi, Z. Selective C-N Borylation of Alkyl Amines Promoted by Lewis Base. *Angew. Chem., Int. Ed.* **2018**, *57*, 15227−15231. (b) Ociepa, M.; Turkowska, J.; Gryko, D. Redox-Activated Amines in $C(sp^3)$-$C(sp)$ and $C(sp^3)$-$C(sp^2)$ Bond Formation Enabled by Metal-Free Photoredox Catalysis. *ACS Catal.* **2018**, *8*, 11362−11367. (c) Sandfort, F.; Strieth-Kalthoff, F.; Klauck, F. J. R.; James, M. J.; Glorius, F. Deaminative Borylation of Aliphatic Amines Enabled by Visible Light Excitation of an Electron Donor-Acceptor Complex. *Chem.—Eur. J.* **2018**, *24*, 17210−17214. (d) Wu, J.; He, L.; Noble, A.; Aggarwal, V. K. Photoinduced Deaminative Borylation of Alkylamines. *J. Am. Chem. Soc.* **2018**, *140*, 10700−10704. (e) James, M. J.; Strieth-Kalthoff, F.; Sandfort, F.; Klauck, F. J. R.; Wagener, F.; Glorius, F. Visible-Light-Mediated Charge Transfer Enables C-C Bond Formation with Traceless Acceptor Groups. *Chem.—Eur. J.* **2019**, *25*, 8240−8244. (f) Jiang, X.; Zhang, M.-M.; Xiong, W.; Lu, L.-Q.; Xiao, W.-J. Deaminative (Carbonylative) Alkyl-Heck-type Reactions Enabled by Photocatalytic C-N Bond Activation. *Angew. Chem., Int. Ed.* **2019**, *58*, 2402−2406. (g) Klauck, F. J. R.; Yoon, H.; James, M. J.; Lautens, M.; Glorius, F. Visible-Light-Mediated Deaminative Three-Component Dicarbofunctionalization of Styrenes with Benzylic Radicals. *ACS Catal.* **2019**, *9*, 236−241. (h) Plunkett, S.; Basch, C. H.; Santana, S. O.; Watson, M. P. Harnessing Alkylpyridinium Salts as Electrophiles in Deaminative Alkyl-Alkyl Cross-Couplings. *J. Am. Chem. Soc.* **2019**, *141*, 2257−2262. (i) Sun, S.-Z.; Romano, C.; Martin, R. Site-Selective Catalytic Deaminative Alkylation of Unactivated Olefins. *J. Am. Chem. Soc.* **2019**, *141*, 16197−16201. (j) Wu, J.; Grant, P. S.; Li, X.; Noble, A.; Aggarwal, V. K. Catalyst-Free Deaminative Functionalizations of Primary Amines by Photoinduced Single-Electron Transfer. *Angew. Chem., Int. Ed.* **2019**, *58*, 5697−5701. (k) Yang, Z.-K.; Xu, N.-X.; Wang, C.; Uchiyama, M. Photoinduced $C(sp^3)$-N Bond Cleavage Leading to the Stereoselective Syntheses of Alkenes. *Chem.—Eur. J.* **2019**, *25*, 5433−5439. (l) Yue, H.; Zhu, C.; Shen, L.; Geng, Q.; Hock, K. J.; Yuan, T.; Cavallo, L.; Rueping, M. Nickel-catalyzed C-N bond activation: activated primary amines as alkylating reagents in reductive cross-coupling. *Chem. Sci.* **2019**, *10*, 4430−4435. (m) Kim, I.; Im, H.; Lee, H.; Hong, S. N-Heterocyclic carbene-catalyzed deaminative cross-coupling of aldehydes with Katritzky pyridinium salts. *Chem. Sci.* **2020**, *11*, 3192−3197. (n) Lübbesmeyer, M.; Mackay, E. G.; Raycroft, M. A. R.; Elfert, J.; Pratt, D. A.; Studer, A. Base-Promoted C-C Bond Activation Enables Radical Allylation with Homoallylic Alcohols. *J. Am. Chem. Soc.* **2020**, *142*, 2609−2616. (o) Wang, C.; Qi, R.; Xue, H.; Shen, Y.; Chang, M.; Chen, Y.; Wang, R.; Xu, Z. Visible-Light-Promoted $C(sp^3)$-H Alkylation by Intermolecular Charge Transfer: Preparation of Unnatural α-Amino Acids and Late-Stage Modification of Peptides. *Angew. Chem., Int. Ed.* **2020**, *59*, 7461−7466. (p) Wang, J.; Hoerrner, M. E.; Watson, M. P.; Weix, D. J. Nickel-Catalyzed Synthesis of Dialkyl Ketones from the Coupling of N-Alkyl Pyridinium Salts with Activated Carboxylic Acids. *Angew. Chem., Int. Ed.* **2020**, *59*, 13484−13489. (q) Zeng, X.; Yan, W.; Zacate, S. B.; Cai, A.; Wang, Y.; Yang, D.; Yang, K.; Liu, W. Copper-Catalyzed Deaminative Difluoromethylation. *Angew. Chem., Int. Ed.* **2020**, *59*, 16398−16403. (r) Cai, Z.; Gu, R.; Si, W.; Xiang, Y.; Sun, J.; Jiao, Y.; Zhang, X. Photoinduced allylic defluorinative alkylation of trifluoromethyl alkenes with Katritzky salts under catalyst- and metal-free conditions. *Green Chem.* **2022**, *24*, 6830−6835.

(12) Berger, K. J.; Driscoll, J. L.; Yuan, M.; Dherange, B. D.; Gutierrez, O.; Levin, M. D. Direct Deamination of Primary Amines via Isodiazene Intermediates. *J. Am. Chem. Soc.* **2021**, *143*, 17366−17373.

(13) Brown, K. L. Chemistry and Enzymology of Vitamin B12. *Chem. Rev.* **2005**, *105*, 2075−2150.

(14) (a) Daikh, B. E.; Finke, R. G. The persistent radical effect: a prototype example of extreme, 105 to 1, product selectivity in a free-radical reaction involving persistent.cntdot.CoII[macrocycle] and alkyl free radicals. *J. Am. Chem. Soc.* **1992**, *114*, 2938−2943. (b) Wang, Y.; Begley, T. P. Mechanistic Studies on CysS - A Vitamin B12-Dependent Radical SAM Methyltransferase Involved in the Biosynthesis of the tert-Butyl Group of Cystobactamid. *J. Am. Chem. Soc.* **2020**, *142*, 9944−9954.

(15) For reviews; (a) Ram Bajya, K.; Selvakumar, S. Dual Photoredox and Cobalt Catalysis Enabled Transformations. *Eur. J. Org Chem.* **2022**, *2022*, No. e202200229. (b) Kojima, M.; Matsunaga, S. The Merger of Photoredox and Cobalt Catalysis. *Trends Chem.* **2020**, *2*, 410−426.

(16) Selected examples: (a) Abrams, D. J.; West, J. G.; Sorensen, E. J. Toward a mild dehydroformylation using base-metal catalysis. *Chem. Sci.* **2017**, *8*, 1954−1959. (b) Cartwright, K. C.; Tunge, J. A. Decarboxylative Elimination of N-Acyl Amino Acids via Photoredox/Cobalt Dual Catalysis. *ACS Catal.* **2018**, *8*, 11801−11806. (c) Sun, X.; Chen, J.; Ritter, T. Catalytic dehydrogenative decarboxyolefination of carboxylic acids. *Nat. Chem.* **2018**, *10*, 1229−1233. (d) Zhao, H.; McMillan, A. J.; Constantin, T.; Mykura, R. C.; Juliá, F.; Leonori, D. Merging Halogen-Atom Transfer (XAT) and Cobalt Catalysis to Override E2-Selectivity in the Elimination of Alkyl Halides: A Mild Route toward contra-Thermodynamic Olefins. *J. Am. Chem. Soc.* **2021**, *143*, 14806−14813. (e) Huang, L.; Ji, T.; Zhu, C.; Yue, H.; Zhumabay, N.; Rueping, M. Bioinspired desaturation of alcohols enabled by photoredox proton-coupled electron transfer and cobalt dual catalysis. *Nat. Commun.* **2022**, *13*, 809. (f) Wang, X.; Li, Y.; Wu, X. Photoredox/Cobalt Dual Catalysis Enabled Regiospecific Synthesis of Distally Unsaturated Ketones with Hydrogen Evolution. *ACS Catal.* **2022**, *12*, 3710−3718. (g) Caldora, H. P.; Zhang, Z.; Tilby, M. J.; Turner, O.; Leonori, D. Dual Photochemical H-Atom Transfer and Cobalt Catalysis for the Desaturative Synthesis of Phenols from Cyclohexanones. *Angew. Chem., Int. Ed.* **2023**, *62*, No. e202301656.

(17) (a) West, J. G.; Huang, D.; Sorensen, E. J. Acceptorless dehydrogenation of small molecules through cooperative base metal catalysis. *Nat. Commun.* **2015**, *6*, 10093. (b) Sahoo, M. K.; Balaraman, E. Room temperature catalytic dehydrogenation of cyclic amines with the liberation of H_2 using water as a solvent. *Green Chem.* **2019**, *21*,

https://doi.org/10.1021/acscatal.3c04305
ACS Catal. 2023, 13, 14205−14212

2119−2128. (c) Zhou, M.-J.; Zhang, L.; Liu, G.; Xu, C.; Huang, Z. Site-Selective Acceptorless Dehydrogenation of Aliphatics Enabled by Organophotoredox/Cobalt Dual Catalysis. *J. Am. Chem. Soc.* **2021**, *143*, 16470−16485. (d) Ritu Kolb, D.; Kolb, D.; Jain, N.; König, B. Synthesis of Linear Enamides and Enecarbamates via Photoredox Acceptorless Dehydrogenation. *Adv. Synth. Catal.* **2023**, *365*, 605−611.

(18) Katritzky, A. R.; El-Mowafy, A. M. Pyrylium-mediated conversion of primary alkyl primary amines into olefins via tetrahydrobenzoacridiniums: a mild alternative to the Hofmann elimination. *J. Org. Chem.* **1982**, *47*, 3506−3511.

(19) (a) Fukuzumi, S.; Kotani, H.; Ohkubo, K.; Ogo, S.; Tkachenko, N. V.; Lemmetyinen, H. Electron-Transfer State of 9-Mesityl-10-methylacridinium Ion with a Much Longer Lifetime and Higher Energy Than That of the Natural Photosynthetic Reaction Center. *J. Am. Chem. Soc.* **2004**, *126*, 1600−1601. (b) Uygur, M.; Danelzik, T.; Mancheño, O. G. Metal-free desilylative C-C bond formation by visible-light photoredox catalysis. *Chem. Commun.* **2019**, *55*, 2980−2983.

(20) Leifert, D.; Studer, A. The Persistent Radical Effect in Organic Synthesis. *Angew. Chem., Int. Ed.* **2020**, *59*, 74−108.

(21) Ng, F. T. T.; Rempel, G. L. Ligand effects on transition metal-alkyl bond dissociation energies. *J. Am. Chem. Soc.* **1982**, *104*, 621−623.

(22) Hari, D. P.; König, B. Synthetic applications of eosin Y in photoredox catalysis. *Chem. Commun.* **2014**, *50*, 6688−6699.

(23) Shang, T.-Y.; Lu, L.-H.; Cao, Z.; Liu, Y.; He, W.-M.; Yu, B. Recent advances of 1,2,3,5-tetrakis(carbazol-9-yl)-4,6-dicyanobenzene (4CzIPN) in photocatalytic transformations. *Chem. Commun.* **2019**, *55*, 5408−5419.

(24) Ramirez, N. P.; König, B.; Gonzalez-Gomez, J. C. Decarboxylative Cyanation of Aliphatic Carboxylic Acids via Visible-Light Flavin Photocatalysis. *Org. Lett.* **2019**, *21*, 1368−1373.

(25) Wang, C.; Azofra, L. M.; Dam, P.; Espinoza-Suarez, E. J.; Do, H. T.; Rabeah, J.; Brückner, A.; El-Sepelgy, O. Photoexcited cobalt catalysed endo-selective alkyl Heck reaction. *Chem. Commun.* **2023**, *59*, 3862−3865.

(26) Wang, C.; Azofra, L. M.; Dam, P.; Sebek, M.; Steinfeldt, N.; Rabeah, J.; El-Sepelgy, O. Catalytic Desaturation of Aliphatic Amides and Imides Enabled by Excited-State Base-Metal Catalysis. *ACS Catal.* **2022**, *12*, 8868−8876.

(27) Fukuzumi, S.; Ohkubo, K.; Suenobu, T.; Kato, K.; Fujitsuka, M.; Ito, O. Photoalkylation of 10-Alkylacridinium Ion via a Charge-Shift Type of Photoinduced Electron Transfer Controlled by Solvent Polarity. *J. Am. Chem. Soc.* **2001**, *123*, 8459−8467.

(28) (a) Ye, J.-H.; Miao, M.; Huang, H.; Yan, S.-S.; Yin, Z.-B.; Zhou, W.-J.; Yu, D.-G. Visible-Light-Driven Iron-Promoted Thiocarboxylation of Styrenes and Acrylates with CO2. *Angew. Chem., Int. Ed.* **2017**, *56*, 15416−15420. (b) Gandeepan, P.; Müller, T.; Zell, D.; Cera, G.; Warratz, S.; Ackermann, L. 3d Transition Metals for C-H Activation. *Chem. Rev.* **2019**, *119*, 2192−2452. (c) Jamatia, R.; Mondal, A.; Srimani, D. Visible-Light-Induced Manganese-Catalyzed Reactions: Present Approach and Future Prospects. *Adv. Synth. Catal.* **2021**, *363*, 2969−2995.

https://doi.org/10.1021/acscatal.3c04305
ACS Catal. 2023, 13, 14205−14212